

# **Combining Polar Hyper-spectral and Geostationary Multi-spectral Sounding Data – A Method to Optimize Sounding Spatial and Temporal Resolution**

**W. L. Smith<sup>1,2</sup>, E. Weisz<sup>1</sup>, and J. McNabb<sup>2</sup>**

<sup>1</sup>University of Wisconsin, Madison WI, USA; <sup>2</sup>Hampton University, Hampton VA, USA

## **Abstract**

A method is developed for combining polar orbiting Direct Broadcast Satellite (DBS) hyper-spectral soundings with geostationary orbiting satellite multi-spectral soundings in order to optimize the spatial and temporal resolution of the derived products. The method is applied to the combination of Direct Broadcast Satellite CrIS and IASI hyper-spectral high vertical resolution sounding data and real-time GOES-16 ABI multi-spectral high horizontal and temporal resolution sounding data. It is shown that the combined sounding products have greater spatial resolution than that provided by either satellite system alone and provide the temporal resolution of the geostationary satellite multi-spectral imager. The intent of the combined DBS polar and geostationary sounding products is to support real-time severe weather forecast applications.

## **1. Introduction**

Polar satellite Hyper-spectral Sounding (PHS) instruments (e.g., AIRS, IASI, and CrIS) are able to provide high vertical resolution temperature and moisture sounding information. This information when received via a Direct Broadcast System (DBS) can be used to monitor the atmospheric stability of the atmosphere for the purpose of predicting where and when severe convective storms may develop (Smith et. al., 2012, Weisz et. al., 2015a, 2015b, 2017). However, the temporal and horizontal resolution of the polar hyper-spectral resolution data is limited for atmospheric stability monitoring application being 12-hr per satellite and 14-km per footprint, respectively. However, the multi-spectral resolution geostationary satellite Advanced Baseline Imager (ABI) contains low vertical resolution water vapor and temperature sounding information but with very high temporal and horizontal resolution, the temporal resolution being as high as 5-min and the horizontal resolution being 2-km. As a result, a method for combining the PHS and ABI data has been developed to optimize the vertical, horizontal, and temporal resolution of the satellite-sounding product.

In particular, the combined polar and geostationary sounding product is intended to be used to: (1) improve low altitude sounding coverage across partly cloudy areas, (2) observe spatial details of atmospheric temperature and moisture important for intense weather prediction, (3) provide high temporal resolution as needed to predict the time of the onset of severe convection, and (4) provide time sequences of altitude-resolved water vapor imagery useful for estimating water vapor feature tracked wind profiles for Numerical Weather Prediction (NWP) applications.

## 2. Satellite Sounding Instrument Measurement Characteristics

Table I shows the measurement characteristics of the polar and geostationary satellite instruments used in this study. As can be seen the spectral resolution of the hyper-spectral polar satellite instruments ranges between  $0.25 \text{ cm}^{-1}$  and  $2.5 \text{ cm}^{-1}$ , depending on spectral band, while the geostationary multi-spectral ABI instrument spectral resolution ranges between  $20 \text{ cm}^{-1}$  and  $140 \text{ cm}^{-1}$ , depending on the spectral channel. However the horizontal resolution for the polar satellite hyper-spectral sounders ranges between 12-km and 14-km while the geostationary satellite multi-spectral resolution ABI is about 2-km, depending on view angle.

**Table I.** Satellite Sounding Instrument Measurement Characteristics

Instrument	AIRS	IASI	CrIS	ABI
Satellite	EOS Aqua	Metop-A, Metop-B	Suomi-NPP, JPSS-1	GOES-16
Type	Grating Spectrometer	Michelson Interferometer	Michelson Interferometer	Radiometer
Spatial resolution (nadir)	13.5 km	12 km	14 km	2 km
Spectral resolution	$0.5 - 2 \text{ cm}^{-1}$	$0.25 \text{ cm}^{-1}$	$0.625 \text{ (LW)}, 1.25 \text{ (MW)}, 2.5 \text{ cm}^{-1} \text{ (SW)}$	$20 - 140 \text{ cm}^{-1}$
Spectral range	$650 - 2670 \text{ cm}^{-1}$ ( $15.4 - 3.7 \text{ }\mu\text{m}$ )	$645 - 2760 \text{ cm}^{-1}$ ( $15.5 - 3.62 \text{ }\mu\text{m}$ )	$650 - 2550 \text{ cm}^{-1}$ ( $15.4 - 3.9 \text{ }\mu\text{m}$ )	$752-21276 \text{ cm}^{-1}$ ( $0.47 - 13.3 \text{ }\mu\text{m}$ )
Number of detectors/ channels	4756 / 2378	12 / 8461	27 / 1305	16 / 16
NEDT range	$0.05 - 0.5 \text{ K}$	$0.1 - 0.75 \text{ K}$	$0.05 - 0.5 \text{ K}$	$0.01 - 0.07 \text{ K}$
Launch year	2002	2006, 2012	2011, 2017	2016

## 3. Methodology

The basis of the retrieval algorithm used for the combined PHS and ABI retrieval methodology is the physically based dual-regression (DR) algorithm. DR is a single Field-of-View (FOV), all-sky condition, retrieval algorithm developed to provide atmospheric soundings, surface and cloud parameters from any of the operational hyper-spectral sounders in real-time from DB Satellite (DBS) sounding radiance spectra (Smith et al. 2012; Weisz et al. 2013). The single FOV and all-sky multiple regression retrieval methodology dates back to the 1980's, having been used before the advent of satellite hyper-spectral instruments for processing airborne hyper-spectral radiance data provided by the HIS (1986-1998), NAST-I (1998–present), and S-HIS (1999–present) aircraft interferometers (see Smith et. el., 2009). Recently, a fast-physical method, based on applying PCRTM (Liu et al. 2006) radiative transfer calculations to numerical forecast model profile data, has been implemented for improving the vertical resolution of vertical resolution aliased regression profile retrievals (Smith and Weisz 2017). The vertically enhanced DR retrievals are hereafter called DRDA retrievals, the DA standing for the vertically De-Aliasing correction step of the retrieval process.

The combined PHS (i.e., AIRS, CrIS, and IASI) with ABI retrieval methodology can be summarized as follows.

- (1) From the portion of a Direct Broadcast System (DBS) polar orbiting satellite hyper-spectral data covering the geographical area of interest (e.g., the mid-Atlantic Virginia/North Carolina region considered here), DRDA retrievals are produced.

Simultaneous with step 1, ABI clear-sky 2-km resolution DR retrievals are produced for the area of interest and for the same time as the polar overpass of that area.

- (2) The next step involves area averaging the ABI retrievals within each FOV of the PHS. The area average ABI retrievals are then used with the PHS retrievals to:
  - a) Produce a regression relation between each PHS retrieval value (e.g., a temperature at a particular altitude) and the ABI retrieval values at 200, 400, 600, 800, and 1000-hPa are used as predictors. These regression relations are then used to enhance the low vertical resolution ABI retrieval product accuracy based on their comparisons to the higher vertical resolution PHS retrievals.
  - b) Next the following formula is used to estimate the PHS retrieval value at the position and time of the ABI data:

$$\text{PHS/ABI}(x,y,t) = \text{ABI}(x,y,t) + [\text{PHS}(x_0,y_0,t_0) - \text{ABI}^*(x_0,y_0,t_0)] \quad (1)$$

where PHS/ABI is the combined PHS and ABI retrieval, ABI is the regression enhanced ABI retrieval obtained in step 1,  $x$ ,  $y$ , and  $t$  are the position and time of the ABI retrieval data,  $x_0$ ,  $y_0$ , and  $t_0$  are the position and time of the PHS retrieval data, and  $\text{ABI}^*$  is the ABI regression retrieval obtained at the PHS observation time over the FOVs of the PHS instrument.

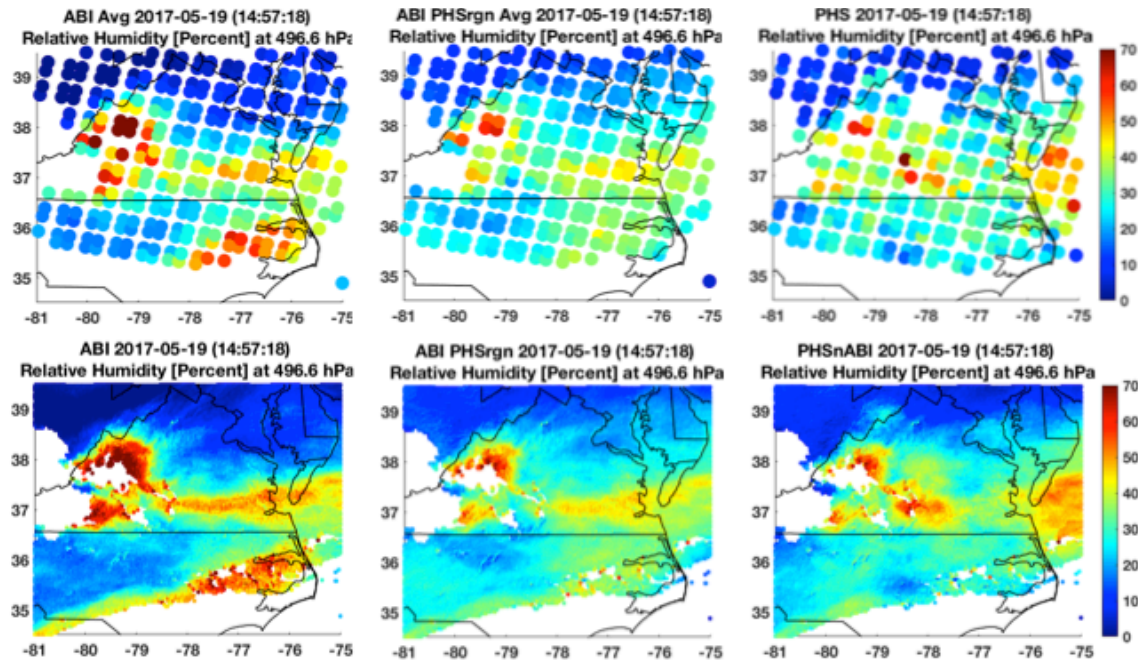
- (3) PHS/ABI retrievals are then obtained for positions and data frames of subsequent ABI data (i.e., for ABI data frames obtained every 30 minutes) until the next PHS overpass occurs when the  $(x_0, y_0, t_0)$  reference values are updated.

#### 4. Results

As an example, Polar Hyper-spectral Satellite (PHS) radiances received by the Hampton University Direct Broadcast System (DBS) have been combined with GOES-16 geostationary ABI data for May 19 and May 22, 2017. On May 19, severe weather, which was not predicted well, occurred across the Hampton Roads area. However, three days later severe weather was predicted for the Hampton Roads area but this severe weather never materialized. It will be shown that for both these cases the stability indices computed from the combined polar and geostationary sounding data would have alerted the forecasters that the operational forecast stability indices were giving a false indication of severe weather development, or lack thereof, for these two days.

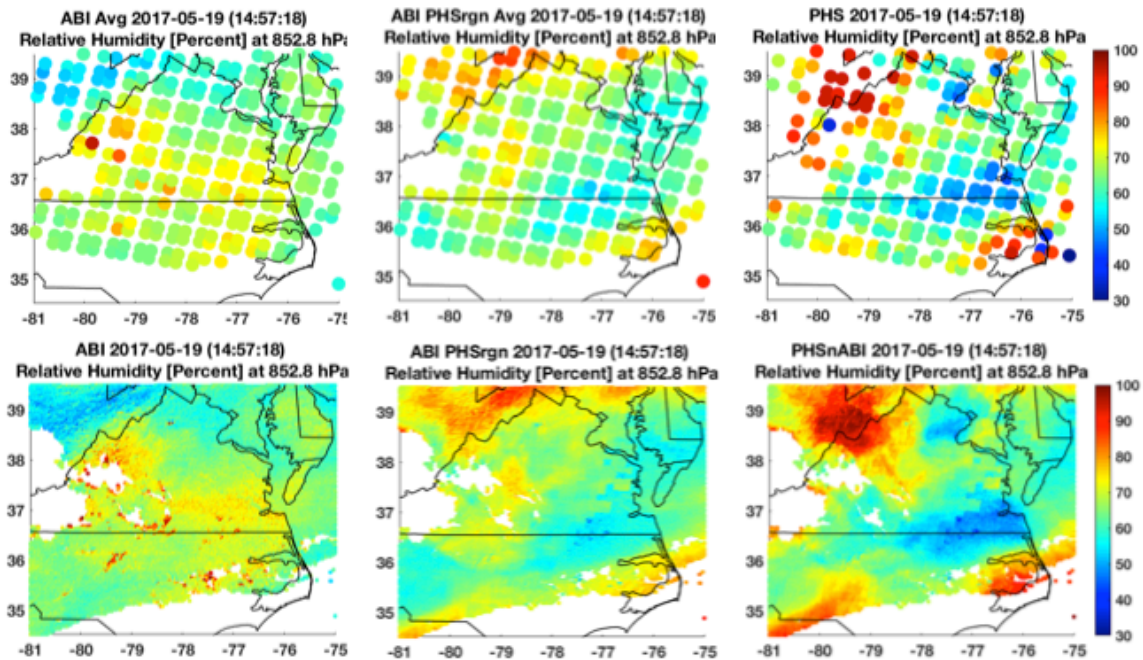
Figure 1 and 2 shows the ABI, PHS, and combined radiances at the first of three polar satellite overpasses of the Hampton Roads region, which occurred about 15 UTC on May 19, 2017. The upper panels of Fig. 1 and 2 show the ABI and PHS 500-hPa and 850-hPa, respectively, relative humidity at the resolution of the PHS (i.e., IASI in this case) measurements, the panel in the middle being the ABI regression predicted PHS sounding values used in Eq. (1) above. It can be seen that significant differences between the ABI and PHS sounding data occur presumably due to their difference in vertical resolution.

However, the lower panels show ABI, ABI regression predicted PHS, and the combined PHS and ABI derived relative humidity values at the horizontal resolution of the ABI. As can be seen by comparing the lower right panels with the upper right panels, the PHS plus ABI product portrays all the PHS high vertical resolution profile features at the high horizontal resolution of the ABI. Thus, the combined PHS and ABI sounding product optimizes the spatial resolution of the sounding product.



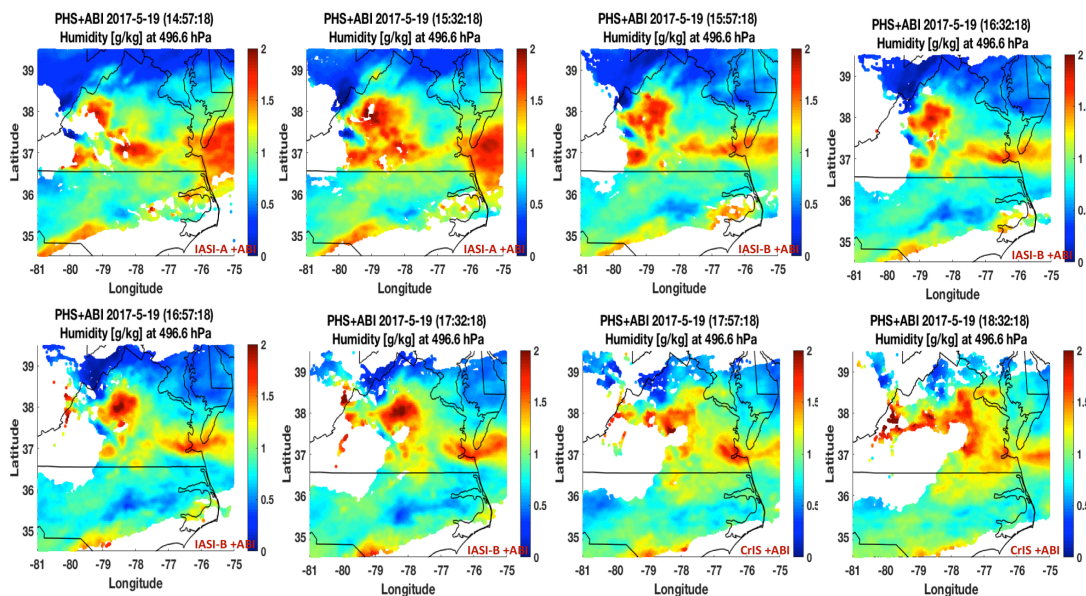
**Figure 1.** ABI, PHS, and combined ABI and PHS 500-hPa relative humidity values at ~15 UTC on May 19, 2017. The upper panels show the ABI and PHS 500-hPa relative humidity at the resolution of the PHS measurements, the panel in the middle being the ABI regression predicted PHS sounding values. The lower panels show ABI, ABI regression predicted PHS humidity values, and the combined PHS and ABI derived 500-hPa relative humidity values at the horizontal resolution of the ABI.

Figure 3 shows the PHS+ABI 500-hPa absolute humidity results obtained for a 30 minute interval time sequence of ABI data combined with the 15 UTC (Metop-A IASI), 16 UTC (Metop-B IASI), and 18 UTC (SNPP-CrIS) PHS DBS data received at Hampton University on May 19, 2017. One can see some small discontinuities between the 30-minute interval images when transitioning from one PHS instrument to the next (i.e., going from IASI-A to IASI-B to CrIS). Thus, it appears to be important to avoid these transition frames within a time sequence of images to be used to compute water vapor motion wind vectors. Such avoidance is easy to do since the ABI has a refresh rate of at least 15 minutes.

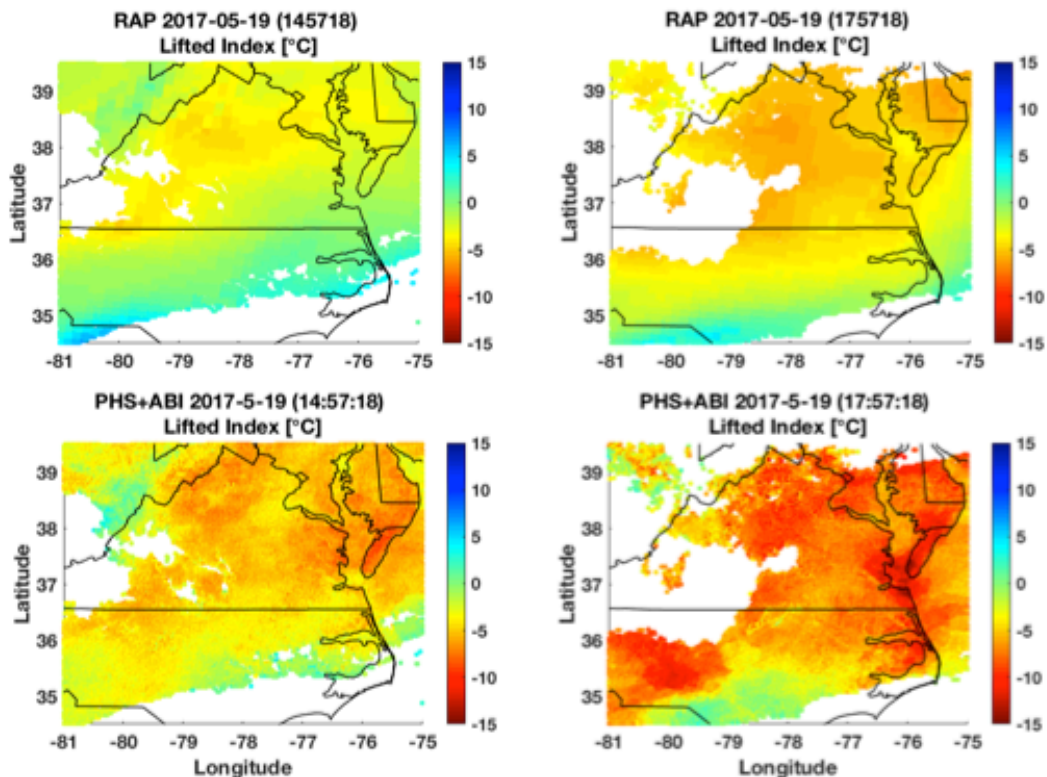


**Figure 2.** Same as Fig. 1 for the 850-hPa level.

With regards to the prediction of severe convection, Fig. 4 shows the Lifted Index provide by the operational RAP model and observed by satellite at two different times on May 19, 2017. As can be seen the satellite measurements indicate a greater degree of instability than does the operational RAP product and a much larger decrease in atmospheric stability between the afternoon and the mid-morning morning, this indicating the potential for severe convection during the afternoon and evening hours on this particular day.

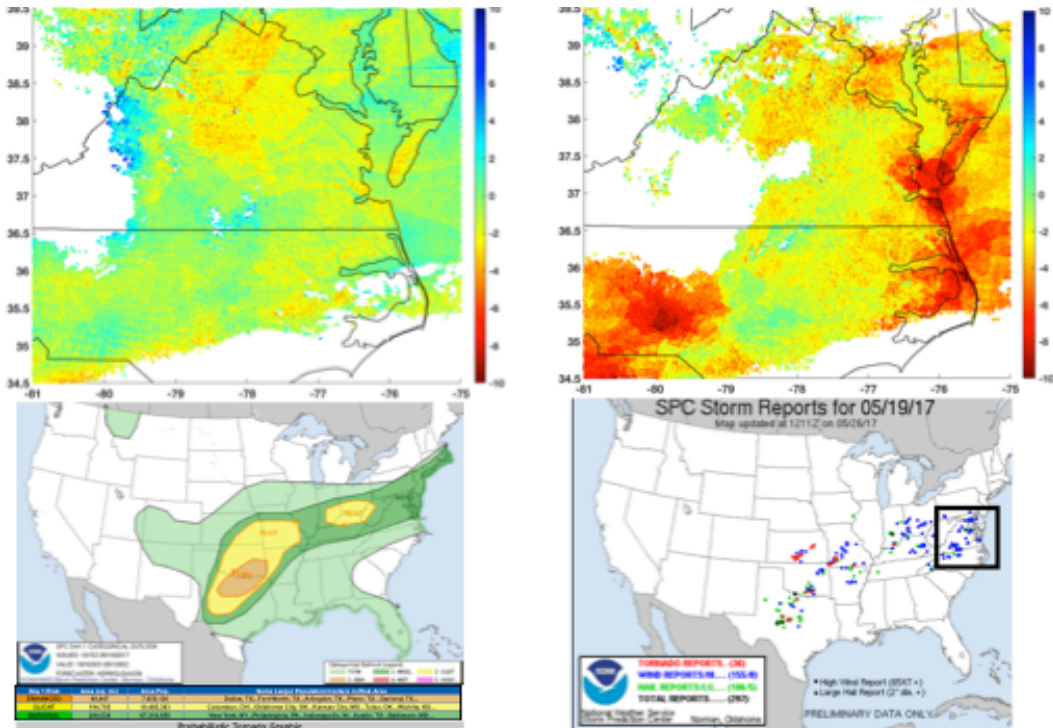


**Figure 3.** 30-minute interval combined ABI+PHS 500-hPa absolute humidity (g/kg) values for May 19, 2017.



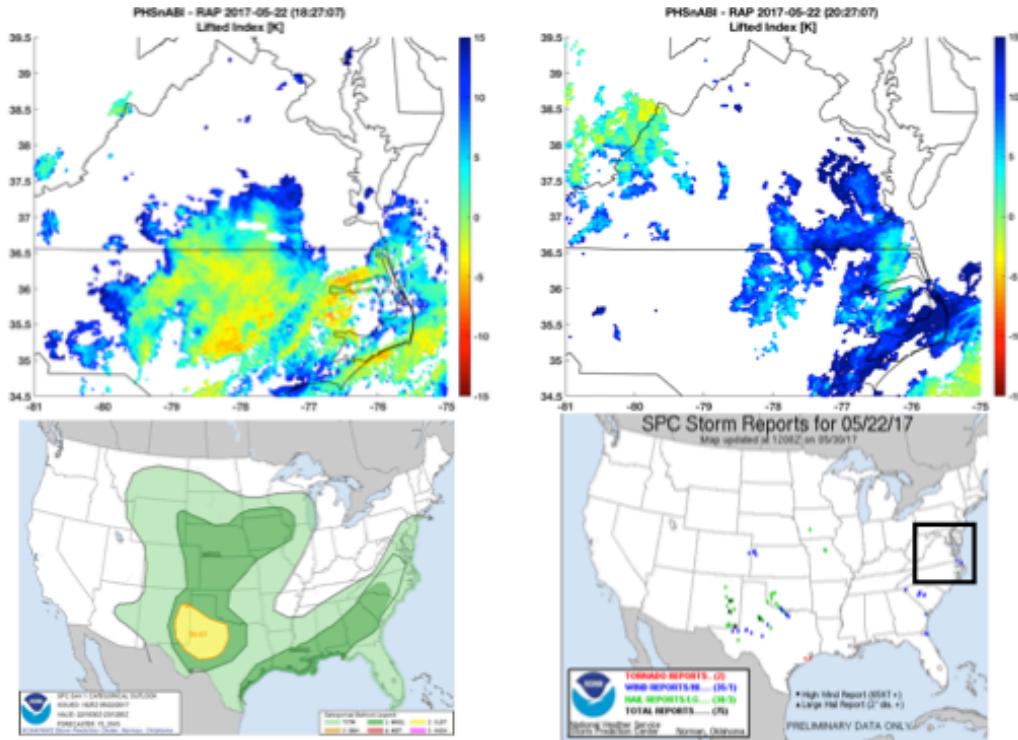
**Figure 4.** Lifted Index stability parameter provided by RAP analysis compared with that measured by the Metop-A IASI and SNPP CrIS instruments at approximately 15 UTC and 18 UTC on May 19, 2017.

Figure 5 shows the time difference between the satellite observed Lifted Index and the RAP analysis of Lifted Index at approximately 16 UTC and 18 UTC on May 19, 2017, respectively (top two panels) together with the outlook for convection (lower left panel) and the surface observed storm reports provided by NOAA's Storm Prediction Center. As can be seen, the operational outlook was revealing only a slight chance for convection within the southeastern Virginia Hampton Roads region whereas the satellite measurements at 18 UTC indicated a much greater chance for severe convective storms occurring than does the operational RAP Lifted Index stability parameter analysis. As shown by the surface observer severe storm reports (lower right panel of Fig. 5), numerous convective storms producing severe winds were produced within the Hampton Roads region during the afternoon and evening hours after the satellite observations provided strong indications that severe convection within this area was likely to occur.



**Figure 5.** The time difference between the satellite observed Lifted Index and the RAP analysis of Lifted Index at approximately 16 UTC and 18 UTC on May 19, 2017, respectively (top two panels) together with the outlook for convection (lower left panel) and the surface observed storm reports provided by NOAA’s Storm Prediction Center.

It is interesting to note that three days later, as shown in Fig. 6, the satellite data once again provided convection indications, which were different than the operational forecast indications for the Hampton Roads Virginia area. However, this time the RAP and Satellite indications for severe convection were in the opposite sense of those indications provided for May 19 2017. As can be seen from Fig. 6, the operational outlook (lower left panel) once again indicated a slight chance for convection across the Hampton Roads and North Carolina regions whereas the satellite data (upper two panels) provided strong indications that convective weather was highly unlikely to occur since the atmospheric stability was increasing with time across the Hampton Roads and North Carolina regions. As can be seen from the lower right panel of Fig. 6, there were no reports of severe convection occurring across the Virginia North Carolina region in good correspondence to the satellite data stability measurement indications shown in the upper panels of Fig. 6.



**Figure 6.** The time difference between the satellite observed Lifted Index and the RAP analysis of Lifted Index at approximately 18:30 UTC and 20:30 UTC on May 19, 2017, respectively (top two panels) together with the outlook for convection (lower left panel) and the surface observed storm reports provided by NOAA’s Storm Prediction Center.

## 5. Summary and Conclusions

Direct Broadcast Satellite (DBS) polar satellite hyper-spectral soundings can be combined with geostationary satellite multi-spectral soundings to provide in real-time high spatial and temporal resolution atmospheric sounding products, which can be used for predicting subsequent intense convection and associated severe storms. In particular, the combined polar and geostationary sounding products can be used to: (1) improve low altitude sounding coverage across partly cloudy areas, (2) observe spatial details of atmospheric temperature and moisture important for intense weather prediction, (3) provide high temporal resolution as needed to predict the time of the onset of severe convection. Also, the resulting time sequences of altitude-resolved water vapor imagery may be useful for estimating water vapor feature tracked wind profiles for Numerical Weather Prediction (NWP) applications. The procedure for combining DBS polar and geostationary satellite sounding observations can be implemented wherever DBS data is available and therefore would make possible quasi-continuous high spatial resolution sounding coverage of the entire CONUS area.

## REFERENCES

- Liu, X., W. L. Smith, D. K. Zhou, and A. M. Larar (2006), Principal Component-based Radiative Transfer Forward Model (PCRTM) For Hyperspectral Sensors, Part I: Theoretical Concept, *Applied Optics*, 201-209, 45.
- Smith, W. L. Sr., H. Revercomb, G. Bingham, A. Larar, H. Huang, D. Zhou, J. Li, X. Liu, and S. Kireev (2009), Evolution, current capabilities, and future advances in satellite ultra-spectral IR sounding *Atmos. Chem. Phys.*, 9, 6541-6569
- Smith, W. L., E. Weisz, S. Kirev, D. K. Zhou, Z. Li, and E. E. Borbas (2012), Dual-Regression Retrieval Algorithm for Real-Time Processing of Satellite Ultraspectral Radiances, *J. Appl. Meteor. Clim.*, vol. 51, no. 8, pp.1455-1476
- Smith, W. L., and E. Weisz. (2017) Dual Regression Approach for High Spatial Resolution Infrared Soundings, in *Comprehensive Remote Sensing*, M. Goldberg, Editor, Elsevier Ltd, Langford Lane Oxford, OX5 1GB UK.
- Weisz, E., Smith, W. L., and N. Smith (2013), Advances in simultaneous atmospheric profile and cloud parameter regression based retrieval from high-spectral resolution radiance measurements. *J. Geophys. Res.-Atm.*, 118, 6433-6443.
- Weisz, E., N. Smith, W. L. Smith (2015a), The use of hyperspectral sounding information to monitor atmospheric tendencies leading to severe local storms. *Earth and Space Science*, 2.
- Weisz, E., W. L. Smith, and N. Smith (2015b) Assessing Hyperspectral Retrieval Algorithms and their Products for Use in Direct Broadcast Applications, 20th International TOVS Study Conference (ITSC-20) proceedings, 28 October - 3 November 2015, Lake Geneva, Wisconsin, USA; paper 3.03 available at <https://cimss.ssec.wisc.edu/itwg/itsc/itsc20/papers/>.
- Weisz, E., W. L. Smith Sr., K. Strabala, A. Huang and N. Smith (2017), Hyperspectral Sounder Derived Severe Weather Indices, 21st International TOVS Study Conference (ITSC-21), 28 November – 5 December 2017, Darmstadt Germany, poster available at [https://cimss.ssec.wisc.edu/itwg/itsc/itsc21/program/posters/11p.05\\_weisz.pdf](https://cimss.ssec.wisc.edu/itwg/itsc/itsc21/program/posters/11p.05_weisz.pdf)